ORDER, DISORDER, AND PHASE TRANSITION IN CONDENSED SYSTEM

Magnetic Ordering Dependence on Iron Ions Distribution in Cu_2FeBO_5 Ludwigite[1]

I. I. Nazarenko[a,*], S. N. Sofronova[a,], and E. M. Moshkina[a,b,***]**

[a] *Kirensky Institute of Physics, Siberian Branch, Russian Academy of Sciences, Krasnoyarsk, 660036 Russia*
[b] *Reshetnev Siberian State University of Science and Technology, Krasnoyarsk, 660037 Russia*
*e-mail: ilnz@live.ru
**e-mail: ssn@iph.krasn.ru
***e-mail: ekoles@iph.krasn.ru
Received December 15, 2017

Abstract—A comparative analysis of the copper and iron ions bonds exchange energies was conducted for various variants of orderings and distributions of iron ions among crystallographic positions in ludwigite Cu_2FeBO_5. Analysis showed that the exchange bonds of iron ions play a key role in the formation of magnetic order. The magnetic ordering strongly depends on the distribution of iron ions among the positions. In the case when the Fe^{3+} is in the same position as in Fe_3BO_5, the most favorable magnetic structure is similar to the magnetic structure of ludwigite Fe_3BO_5. In other cases, the type of magnetic ordering is different.

1. INTRODUCTION

Recently, thanks to various interesting properties that various composition ludwigites demonstrate [1] much attention has been paid to the studies of them. In monometallic ludwigites, there is a charge ordering—in the Fe_3BO_5 [2, 3]—transition to the low-spin state of a trivalent cobalt ion—in the Co_3BO_5 [4]. Interestingly, in heterometallic ludwigites, a nonmetallic ion also affects the magnetic properties, and if in $Co_5Ti(BO_5)_2$ the state of the spin glass is observed [5], then in $Co_5Sn(BO_5)_2$ transition to a magnetically ordered state is observed at a sufficiently high temperature (84 K) [6, 7]. A great influence on the magnetic properties of ludwigites is exerted not only by the composition but also by the distribution of magnetic ions over the crystallographic positions, which are 4 in the structure of ludwigite Fig. 1).

Previously, Cu_2FeBO_5 was studied by three different groups: it was grown by Bluhm [8] for the first time, however, apart from the crystal structure, other physical properties were not investigated. Later, the Brazilian team had grown and investigated powder samples of Cu_2FeBO_5 [9]. The magnetization curves revealed two features at 68 and 38 K. The first feature, authors [9] associated with the ordering in the iron subsystem since changes in the Mossbauer spectra are observed in this region. At 38 K, no changes are

observed in the Mossbauer spectra, and it was assumed that at this temperature, ordering takes place in the copper subsystem.
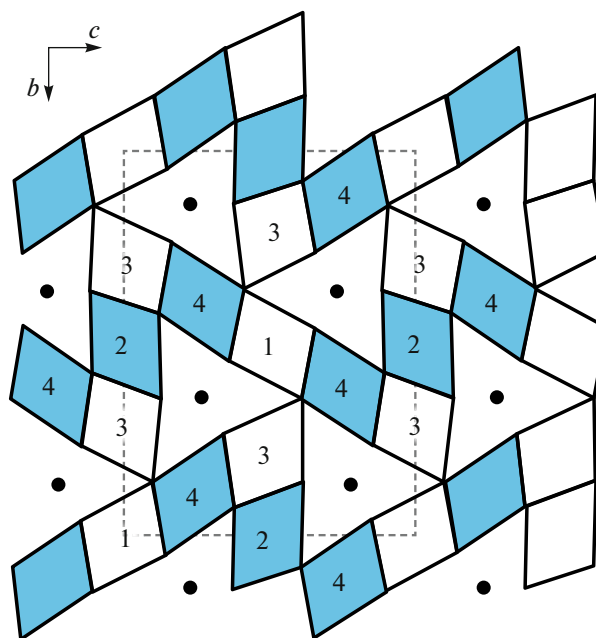
Fig. 1. (Color online) The view of the Cu_2FeBO_5 ludwigite structure in the *bc* plane with the designation of crystallographic positions (1—2b, 2—2c, 3—4e$_1$, 4—4e$_2$), oxygen octahedra, metal ions are located in their centers, black circles are boron ions.

[1] The article is published in the original.

Table 1. Crystallographic positions and numbers of atoms in the unit and doubled along the short axis cell

Unit cell		Double cell	
pos.	atomic number and coordinates	pos.	atomic number and coordinates
2b	1 $(1/2, 0, 0)$, 2 $(1/2, 1/2, 1/2)$	$4e_3$	1 (x, y, z), 1' $(-x, -y, -z)$, 2 $(x, -y + 1/2, z + 1/2)$, 2' $(-x, y + 1/2, -z + 1/2)$
2c	3 $(0, 1/2, 0)$, 4 $(0, 0, 1/2)$	2c 2d	3 $(0,1/2,0)$, 4 $(0,0,1/2)$ 3' $(0,1/2,0)$, 4' $(0,0,1/2)$
$4e_1$	5 $(-x, -y, -z)$, 6 (x, y, z), 7 $(-x, y + 1/2, -z + 1/2)$, 8 $(x, -y + 1/2, z + 1/2)$	$4e_1$ $4e_{1'}$	5 $(-x, -y, -z)$, 6 (x, y, z), 7 $(-x, y + 1/2, -z + 1/2)$, 8 $(x, -y + 1/2, z + 1/2)$ 5' $(-x, -y, -z)$, 6' (x, y, z), 7' $(-x, y + 1/2, -z + 1/2)$, 8' $(x, -y + 1/2, z + 1/2)$
$4e_2$	9 (x, y, z), 10 $(-x, -y, -z)$, 11 $(-x, y + 1/2, -z + 1/2)$, 12 $(x, -y + 1/2, z + 1/2)$	$4e_2$ $4e_{2'}$	9 (x, y, z), 10 $(-x, -y, -z)$, 11 $(-x, y + 1/2, -z + 1/2)$, 12 $(x, -y + 1/2, z + 1/2)$ 9' $(-x, -y, -z)$, 10' (x, y, z), 11' $(-x, y + 1/2, -z + 1/2)$, 12' $(x, -y + 1/2, z + 1/2)$

Authors [9] note that two- and trivalent subsystems do not practically interact with each other down to the lowest temperatures. Below 20 K, features appear on the Mossbauer spectra, which may indicate the interaction of subsystems. Other experimental studies do not support this information.

Later, the Russian group [10] grown Cu_2FeBO_5 single crystal, magnetic properties were also studied. Unlike [9], only one magnetic transition was detected at 31 K. Conducted by the authors [10] a study of the Mossbauer spectra gave the basis for suggesting another model of the iron ions distribution over crystalline positions. The difference in the distribution of iron ions over crystalline positions was explained by the difference in the magnetic properties of Cu_2FeBO_5, grown by various groups [9, 10]. In our work, within the framework of a simple empirical model of Anderson−Zavadsky, we will analyze the exchange interactions for a different distribution of the iron ion over the crystallographic positions. We analyzed the possible magnetic structures and tried to explain the observed differences in the magnetic properties.

2. STRUCTURE AND GROUP-THEORETICAL ANALYSIS

The crystal structure of the ludwigite belongs to the space group *Pbam*, but copper ludwigite refers to a distorted monoclinic variant with space group $P2_1/c$ because of the strong Yahn-Teller effect [9].

As already noted, in the structure of ludwigite, the metallic ion occupies 4 crystallographic positions [1]. In the $P2_1/c$ structure, the symmetrical positions of metallic ions are as follows: 1—2b, 2—2c, 3—$4e_1$, and 4—$4e_2$. In most ludwigites, the trivalent ion predominantly occupies position 4 ($4e_2$), often also can be in position 2 (2c). The geometry of the ludwigite structure is such that the ions in positions 4−2−4 and 3−1−3 form two magnetic subsystems, similar to the three-legged ladders (e.g., Fe_3BO_5 [2, 3] or Cu_2MnBO_5 [11]). Magnetic moments in these subsystems can be oriented not collinear, also ordering in each of these subsystems can occur at different temperatures [3].

To analyze the possible types of magnetic ordering, we carried out group-theoretical analysis. For present symmetry group, we have already carried out group-theoretic analysis for a magnetic cell that coincides with a crystallographic one [11]. Since in the compound that we are investigating, there is an iron ion 3+, which is characterized by strong antiferromagnetic exchanges, leading to doubling the magnetic cell along the short axis in ludwigite Fe_3BO [2, 3], in this paper we performed group-theoretical analysis for a doubled cell.

In both cases, the space group remains $P2_1/c$. Decomposition into irreducible representations for each position:

$$D = 15\tau_1 + 21\tau_2 + 15\tau_3 + 21\tau_4.$$

In Fig. 1, the crystallographic positions of ions in the unit cell are indicated, and in Table 1, the symmetrical positions and ion numbers are given, which are referred to the unit and doubled cells (dashed).

Table 2. The eigenvectors for the irreducible representations for the cell doubled along the short axis of the Cu_2FeBO_5

Pos.	Atom no.	τ_1	τ_2	τ_3	τ_4
$4e_3$	1	$-x, -y, -z$	x, y, z	$-x, -y, -z$	x, y, z
	2	$-x, y, -z$	$-x, y, -z$	$x, -y, z$	$x, -y, z$
	1'	x, y, z	x, y, z	x, y, z	x, y, z
	2'	$x, -y, z$	$-x, y, -z$	$-x, y, -z$	$x, -y, z$
2c	3		x, y, z		x, y, z
	4		$-x, y, -z$		$x, -y, z$
2d	3'		x, y, z		x, y, z
	4'		$-x, y, -z$		$x, -y, z$
$4e_1$	5	x, y, z	x, y, z	x, y, z	x, y, z
	6	$-x, -y, -z$	x, y, z	$-x, -y, -z$	x, y, z
	7	$x, -y, z$	$-x, y, -z$	$-x, y, -z$	$x, -y, z$
	8	$-x, y, -z$	$-x, y, -z$	$x, -y, z$	$x, -y, z$
$4e_{1'}$	5'	x, y, z	x, y, z	x, y, z	x, y, z
	6'	$-x, -y, -z$	x, y, z	$-x, -y, -z$	x, y, z
	7'	$x, -y, z$	$-x, y, -z$	$-x, y, -z$	$x, -y, z$
	8'	$-x, y, -z$	$-x, y, -z$	$x, -y, z$	$x, -y, z$
$4e_2$	9	x, y, z	x, y, z	x, y, z	x, y, z
	10	$-x, -y, -z$	x, y, z	$-x, -y, -z$	x, y, z
	11	$x, -y, z$	$-x, y, -z$	$-x, -y, -z$	$x, -y, z$
	12	$-x, y, -z$	$-x, y, -z$	x, y, z	$x, -y, z$
$4e_{2'}$	9'	x, y, z	x, y, z	x, y, z	x, y, z
	10'	$-x, -y, -z$	x, y, z	$-x, -y, -z$	x, y, z
	11'	$x, -y, z$	$-x, y, -z$	$-x, y, -z$	$x, -y, z$
	12'	$-x, y, -z$	$-x, y, -z$	$x, -y, z$	$x, -y, z$

In Table 2, eigenvectors for each irreducible representation are given for a doubled cell. The magnetic moment for all representations can have all 3 components. The appearance of a partial magnetic order, as described in [9] can be associated with representations τ_1 and τ_3. However, in work [9] at the first transition, the ordering of ions in positions $4e_1$ and 2c, in one of the three-legged stairs was suggested. In accordance with the group-theoretic analysis, partial ordering with respect to irreducible representations τ_1 and τ_3 refers to positions $4e_1$ and $4e_2$.

The appearance of magnetic order on all magnetic ions can be associated with representations τ_2 and τ_4. Depending on the orientation of the magnetic moments, both ferromagnetic and antiferromagnetic ordering can be observed. Complete magnetic ordering can occur within a single transition, as in [11]. In addition, two magnetic transitions can be observed when only one of the eigenvector component is active, as in the compound Fe_3BO_5 [2, 3]. In reality, the picture can be more complicated, since the Cu_2FeBO_5 crystal is not chemically ordered, iron ions are not in only one position (they are in two: 2c and $4e_1$, according to work [8] and in all four positions, according to work [10]). In this case, the symmetry principles will be violated, however, to obtain the basic model of the magnetic order, one can use the obtained data of the group-theoretical analysis.

Table 3. Expressions of the exchange integrals depending on the types of interacting ions (α, β—angles of exchange bonds) between metallic ions through oxygen ligands)

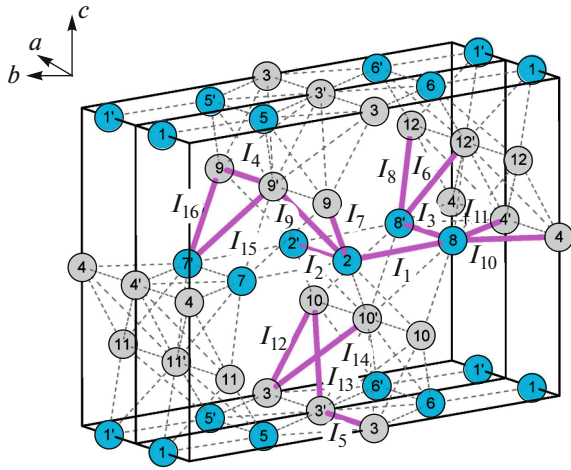|	Superexchange integral
J^{Cu-Cu}	$I_1 = b\left[cJ_{Cu}\sin\alpha + b\left(\frac{1}{3}J_{Cu} - U_{Cu}\right)\lvert\cos\alpha\rvert\right]$
	$I_{2, 3, 4, 5, 6, 7, 11, 12} = bcJ_{Cu}(\sin\alpha + \sin\beta)$
	$I_{8, 9, 10} = 2bcJ_{Cu}(\sin\alpha + \sin\beta)$
	$I_{13} = 0$
	$I_{14} = \frac{1}{3}b^2(2J_{Cu} - 3U_{Cu})\lvert\cos\alpha\rvert$
	$I_{15} = J_{Cu}b\left(\frac{4}{3}b\lvert\cos\alpha\rvert + c\sin\alpha\right)$
	$I_{16} = b\left[b\left(-U_{Cu} + \frac{1}{3}J_{Cu}\right)\sin\alpha + 2cJ_{Cu}\lvert\cos\alpha\rvert\right]$
$J^{Fe^{3+}-Fe^{3+}}$	$I_1 = -\frac{2}{25}U_{Fe}(5\sin\alpha + \lvert\cos\alpha\rvert)$
	$I_{2, 3, 4, 5, 6, 7, 11, 12} = -\frac{4}{3}cU_{Fe}(3b + c)(\sin\alpha + \sin\beta)$
	$I_{8, 9, 10} = -\frac{5}{9}cU_{Fe}(8b + 3c)(\sin\alpha + \sin\beta)$
	$I_{13} = -\frac{1}{27}U_{Fe}(b^2 + 18c^2)\lvert\cos\alpha\rvert$
	$I_{14} = -\frac{2}{9}U_{Fe}(8b^2 + 9c^2)\lvert\cos\alpha\rvert$
	$I_{15, 16} = -\frac{1}{18}U_{Fe}\left[c(8b + 3c)\sin\alpha + 2\left(\frac{8}{3}b^2 + 3c^2\right)\lvert\cos\alpha\rvert\right]$
$J^{Fe^{3+}-Cu}$	$I_1 = \frac{1}{2}\left\{c\left[b\left(\frac{2}{3}J_{Cu} - U_{Fe} - U_{Cu}\right) + J_{Cu}(b + c)\right]\sin\alpha + \left[2J_{Cu}\left(\frac{2}{9}b^2 + c^2\right) - \frac{4}{3}b^2(U_{Cu} + U_{Fe})\right]\lvert\cos\alpha\rvert\right\}$
	$I_{2, 3, 4, 5, 7, 11, 12} = c\left[\left(J_{Cu}\left(\frac{5}{3}b + c\right) - b(U_{Cu} + U_{Fe})\right)\sin\alpha + J_{Cu}\left(\frac{8}{3}b + c\right)\right]\sin\beta$
	$I_6 = cJ_{Cu}\left(\frac{8}{3}b + c\right)(\sin\alpha + \sin\beta)$
	$I_{8, 9, 10} = \left[cJ_{Cu}\left(\frac{5}{3}b + c\right) - bc(U_{Cu} + U_{Fe})\right](\sin\alpha + \sin\beta)$
	$I_{13} = \left(\frac{1}{9}b^2 + 2c^2\right)J_{Cu}\lvert\cos\alpha\rvert$
	$I_{14} = \left[-\frac{4}{3}b^2(U_{Cu} + U_{Fe}) + \left(\frac{4}{9}b^2 + c^2\right)J_{Cu}\right]\lvert\cos\alpha\rvert$
	$I_{15} = \frac{1}{2}J_{Cu}\left[c\left(\frac{8}{3}b + c\right)\sin\alpha + 2\left(\frac{8}{9}b^2 + c^2\right)\lvert\cos\alpha\rvert\right]$
	$I_{16} = \frac{1}{2}\left\{c\left[J_{Cu}\left(\frac{5}{3}b + c\right) - b(U_{Cu} + U_{Fe})\right]\sin\alpha + \left(-\frac{5}{3}b^2(U_{Cu} + U_{Fe}) + \left(\frac{1}{9}b^2 + 2c^2\right)J_{Cu}\right)\lvert\cos\alpha\rvert\right\}$

Fig. 2. (Color online) Exchange paths in the unit cell of Cu_2FeBO_5.

3. METHOD OF CALCULATION

To determine the possible type of magnetic ordering and the exchange integrals values in Cu_2FeBO_5 we used a simple model of indirect coupling [12], based on the theory of superexchange interaction of Anderson and Sawadtzky [13, 14], and Eremin [15]. Indirect exchange interactions Me−O−Me, where Me−Fe or Cu, are schematically depicted in Fig. 2 and denoted by I_i. Unlike other ludwigites, (e.g., Fe_3BO_5) in Cu_2FeBO_5 the crystal cell is monoclinic. Monoclinic distortions are caused by the presence of a Yahn-Teller's copper ion in the cell.

The lowering of the symmetry from rhombohedral to monoclinic leads to an increase of the exchange paths number, compared with the "classical" ludwigites. For example, the exchange interaction between ions 3 and 10 are different from the exchange interaction between ions 3 and 10', whereas in Fe_3BO_5 they are the same.

To analyze the various variants of the iron ions distribution over crystallographic positions, we needed to calculate four types of all exchange interactions paths pairs: Cu−Cu, Fe−Fe, Cu−Fe, Fe−Cu. The formulas for calculating the integrals of indirect exchange interactions are given in Table 3. In the calculations, we used the following parameters: $b = 0.02$, $c = 0.01$, where b and c are the parameters of ligand−cation electron transfer for π and σ bonds, $U_{Cu} = 2.2$ eV, $U_{Fe^{3+}} = 4.5$ eV—excitation energies of the ligand−cation, $J_{Cu} = 1.7$ eV, $J_{Fe^{3+}} = 3$ eV—integral of intraatomic exchange [16].

The calculated values of the exchange integrals, as well as the angles of the bonds Me−O−Me are shown in Table 4. The most significant contribution to the energy is provided by the antiferromagnetic interactions of Fe−Fe, in spite of the fact that the magnitude of the exchange is smaller, the $s_{Fe^{3+}} = 5/2$ spin is five times higher than in copper. The exchange interac-

Table 4. The exchange interaction for various Cu_2FeBO_5 compositions ($N_{i,j}$—crystallographic positions in the unit cell)

	N_i	N_j	α	β	J^{Cu-Cu}, K	$J^{Fe^{3+}-Fe^{3+}}$, K	$J^{Cu-Fe^{3+}}$, K	$J^{Fe^{3+}-Cu}$, K
I_1	3	1	120.0°	−	−0.3	−2.1	−4.6	−4.6
I_2	1	1	90.0°	90.0°	7.9	−5.3	1.1	1.1
I_3	3	3	90.0°	90.0°	7.9	−5.3	1.1	1.1
I_4	4	4	90.0°	100.0°	7.8	−5.2	1.1	1.1
I_5	2	2	90.0°	90.0°	7.9	−5.3	1.1	1.1
I_6	4	3	96.0°	101.0°	7.8	−5.2	4.9	−2.8
I_7	4	1	86.0°	98.9°	7.8	−5.3	1.1	1.1
I_8	4	3	97.0°	98.0°	15.6	−5.2	−2.8	−2.8
I_9	4	1	98.3°	96.0°	15.7	−5.2	−2.8	−2.8
I_{10}	3	2	97.0°	99.0°	15.6	−5.2	−2.8	−2.8
I_{11}	3	2	89.0°	93.0°	7.9	−5.3	1.1	1.1
I_{12}	4	2	100.0°	73.0°	7.9	−5.3	1.1	1.1
I_{13}	4	2	165.0°	−	0.0	−1.0	0.9	0.9
I_{14}	4	2	162.0°	−	−14.5	−3.6	−6.5	−6.5
I_{15}	4	3	120.0°	−	4.4	−2.1	2.0	−2.3
I_{16}	4	3	113.0°	−	0.6	−2.0	−2.5	−1.5
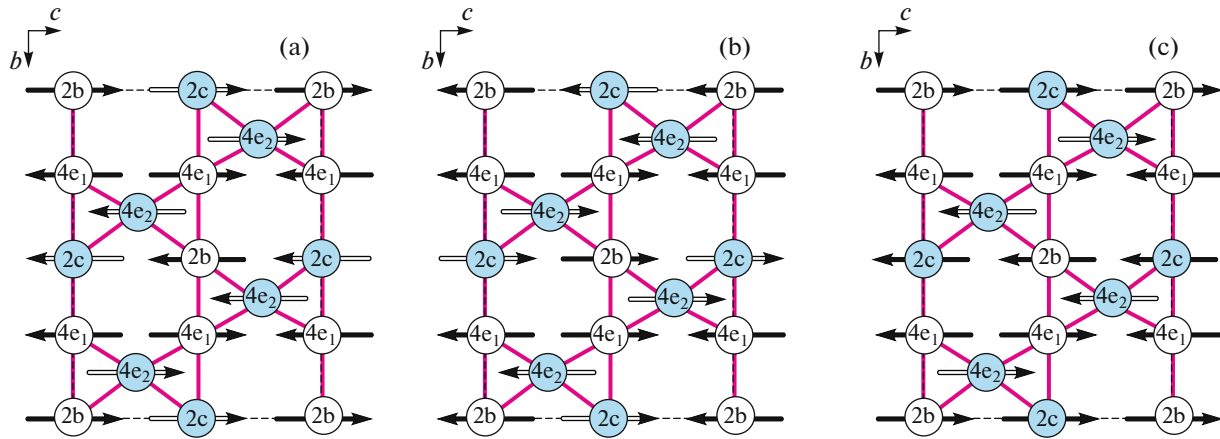
Fig. 3. (Color online) The most energetically favorable structures for composition 1: (a) AFM2, (b) AFM1, (c) AFM3 (solid arrows show the FM orientation of the moments along the *a* axis, the dashed arrows show the AFM orientation of the moments along the *a* axis).

tions of Cu–Cu are ferrimagnetic, with the exception of the 180° exchange interaction I_{14} and 120° exchange interaction J_1.

According to the rule of Goodinax–Kanamori [17] 90°, the Fe–Cu exchange interaction is weak, which is confirmed by our calculations.

After the values of the exchange interactions were obtained, we calculated the energies within the framework of the simple Ising model: $E = -\frac{1}{2}\Sigma I_{ij}s_i s_j$, for various distributions of iron ions over crystallographic positions.

In the first case we considered the "classical" ludwigite, when the trivalent ion occupies only position 4. In the second case, we considered a composition in which the distribution of iron ions corresponds to that obtained in the work [8], in the third case, the distribution of iron ions was, as in the work [10]. Summary data on the filling with copper and iron ions of different positions are given in Table 5.

As we have already noted, a characteristic feature of ludwigite is the subdivision into two subsystems (three-legged ladders). Magnetic moments in subsystems can be collinear (Co$_3$BO$_5$ [4]), directed at the

Table 5. Occupation of the crystallographic positions for various Cu$_2$FeBO$_5$ compositions

Pos.	Comp. 1		Comp. 2 [8]		Comp. 3 [10]	
	Fe	Cu	Fe	Cu	Fe	Cu
2b	0	1	0	1	0.48	0.52
2c	0	1	0.4	0.6	0.98	0.02
4e$_1$	0	1	0	1	0.01	0.99
4e$_2$	1	0	0.8	0.2	0.25	0.75

angle of 60° (Cu$_2$MnBO$_5$ [11]) and 90° (Fe$_3$BO$_5$ [2, 3]). We tried to simulate this situation.

We carried out the calculation for both a cell: coinciding with a crystallographic cell and a cell doubled along a short axis. We chose this type of cell doubling, since the antiferromagnetic interactions 4e$_1$–4e$_1$ and 2c–2c, when in position 4e$_1$ and 2c are iron ions. In the compositions studied by us, iron ions occupy predominantly either position 4e$_1$ (composition 1 and composition 2 [8]), or position 2c (composition 3 [10]).

We present the calculated energy per formula unit so that it is convenient to compare. The energies of magnetically ordered structures that coincide with the crystallographic structure are represented in Table 6.

As can be seen from Tables 7–9, the unit cells doubled along the short axis are more favorable, apparently, one should expect that in Cu$_2$FeBO$_5$ the magnetic cell will be doubled relative to the crystallographic one.

The type of magnetic ordering depends on the composition. In the composition 1, when the iron ions 3+ are located exclusively in position 4e$_1$, in the case where the directions of the magnetic moments in the subsystems 1 and 2 are collinear, at once all 3 magnetic structures have a very close energy (Fig. 3).

The structure depicted in Fig. 3a is very similar to the one obtained by Bordet [3] for Fe$_3$BO$_5$, however, in Fe$_3$BO$_5$ both pairs of three-legged ladders in subsystems 1 and 2 have the same direction of magnetic moments. In the same case, the magnetic moments in the three-legged ladders of the same type are oriented in the opposite direction. Magnetic structure Fig. 3b differs only in the direction of the magnetic moments at position 2b, but since the exchange interaction of 2b–4e$_2$ is very weak, it practically does not contribute to the energy.

Table 6. The energies (in Kelvin) of magnetically ordered Cu_2FeBO_5 structures of different composition for the collinear orientation of the magnetic moments in the subsystems 1 and 2 relative to each other for a cell coinciding with the crystallographic one (FIM is the ferrimagnetic phase)

2b	2c	4e$_1$	4e$_2$	Type	E (Comp. 1), K	E (Comp. 2 [8]), K	E (Comp. 3 [10]), K
↑↑	↓↓	↑↑↑↑	↑↑↑↑	FIM1	186	25	−89
		↑↓↑↓	↑↓↑↓	FIM2	184	43	−88
↓↑	↓↑	↑↑↓↓	↑↑↓↓	AFM1	147	7	−85
		↑↓↓↑	↑↓↓↑	FIM3	145	26	−76
↑↑	↑↑	↑↑↑↑	↑↑↑↑	FM	183	9	−53
↓↓	↓↓	↑↑↑↑	↑↑↑↑	FIM4	168	53	−14
↓↑	↓↑	↓↓↑↑	↓↓↑↑	AFM2	131	36	5
↑↑	↓↓	↓↓↓↓	↓↓↓↓	FIM5	166	36	22
		↓↑↑↓	↑↓↓↑	FIM6	101	53	24
		↓↑↓↑	↑↓↑↓	FIM7	62	36	35
↑↓	↑↓	↑↑↓↓	↓↓↑↑	AFM3	56	−35	36
↑↓	↑↓	↑↑↓↓	↑↓↑↓	AFM4	92	−7	39
↑↑	↓↓	↓↓↓↓	↑↑↑↑	AFM5	17	−53	40
↑↓	↑↓	↑↑↓↓	↑↑↓↓	AFM6	128	20	41
↑↓	↓↑	↑↑↓↓	↓↓↑↑	AFM7	147	88	46
↑↑	↑↑	↓↓↓↓	↑↑↑↑	FIM8	108	70	50
↑↓	↓↑	↓↓↑↑	↑↑↓↓	AFM8	38	−7	111
↓↑	↓↑	↑↑↓↓	↓↓↑↑	AFM9	130	116	121
↑↑	↑↑	↑↑↑↑	↓↓↓↓	FIM9	1	−24	130
↑↑	↓↓	↑↑↑↑	↓↓↓↓	AFM10	92	99	140

Table 7. The energies (in Kelvin) of magnetically ordered Cu_2FeBO_5 structures of composition 1 with different orientations of the magnetic moments in the subsystems 1 and 2 relative to each other

2c	2d	4e$_1$	4e$_{1'}$	4e$_2$	4e$_{2'}$	4e$_3$	Type	E (0°), K	E (60°), K	E (90°), K
↑↓	↓↑	↓↓↑↑	↓↓↑↑	↑↑↓↓	↓↓↑↑	↓↑↓↑	AFM1	−172	−172	−172
↓↑	↑↓	↓↓↑↑	↓↓↑↑	↓↓↑↑	↑↑↓↓	↑↓↑↓	AFM2	−172	−172	−172
↓↑	↓↑	↓↓↑↑	↓↓↑↑	↓↓↑↑	↑↑↓↓	↑↓↑↓	AFM3	−170	−159	−147
↑↓	↓↑	↓↓↑↑	↓↓↑↑	↓↓↑↑	↓↓↑↑	↑↓↑↓	AFM4	147	143	139
↑↓	↓↑	↓↓↑↑	↓↓↑↑	↓↓↑↑	↓↓↑↑	↑↓↑↓	AFM5	153	138	123
↑↑	↓↓	↑↑↑↑	↑↑↑↑	↑↑↑↑	↑↑↑↑	↑↑↑↑	FIM	192	158	123

Table 8. The energies (in Kelvin) of magnetically ordered Cu_2FeBO_5 structures of composition 2 [8] with different orientations of the magnetic moments in the subsystems 1 and 2 relative to each other

2c	2d	4e$_1$	4e$_{1'}$	4e$_2$	4e$_{2'}$	4e$_3$	Type	E (0°), K	E (60°), K	E (90°), K
↑↓	↓↑	↓↓↑↑	↓↓↑↑	↑↑↓↓	↓↓↑↑	↓↑↓↑	AFM1	−74	−74	−74
↓↑	↑↓	↓↓↑↑	↓↓↑↑	↓↓↑↑	↑↑↓↓	↑↓↑↓	AFM2	−75	−75	−75
↓↑	↓↑	↓↓↑↑	↓↓↑↑	↓↓↑↑	↑↑↓↓	↑↓↑↓	AFM3	−103	−86	−68
↑↓	↓↑	↓↓↑↑	↑↑↓↓	↓↓↑↑	↓↓↑↑	↑↓↑↓	AFM4	46	53	60
↑↓	↓↑	↓↓↑↑	↓↓↑↑	↓↓↑↑	↓↓↑↑	↑↓↑↓	AFM5	16	30	44
↑↑	↓↓	↑↑↑↑	↑↑↑↑	↑↑↑↑	↑↑↑↑	↑↑↑↑	FIM	34	39	44
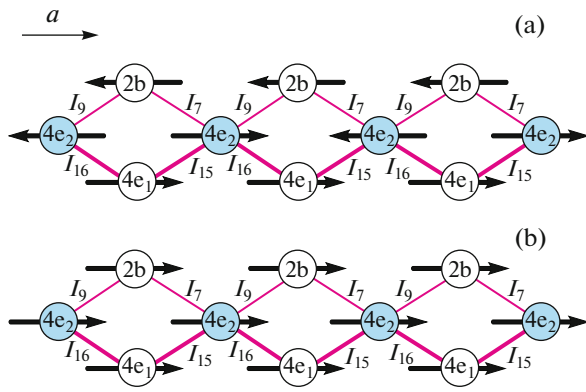
Fig. 4. (Color online) Weak influence of the exchange interactions of position 2b on the ordering of neighboring ions.

It should be noted that with the rotation of the magnetic moments of subsystem 1 relative to subsystem 2, the energy of these magnetic structures does not change, this is due to the geometric features of the ludwigite structure: in the case when the moments in position $4e_1$ are ordered antiferromagnetically along the short axis a, and in positions $4e_2$ and 2b are ferromagnetic, the exchange interactions $4e_1$–$4e_2$ and $4e_1$–2b are completely compensated (Fig. 4). And since the interaction $4e_2$–2b is very weak, it is possible that the magnetic moments in position 2b are ordered only at the lowest temperatures, or they do not order at all.

The energy of the magnetic structure Fig. 3c depends very strongly on the orientation of the magnetic moments of the subsystems relative to each other. This is due to the fact that the magnetic moments in positions 2c and $4e_2$ are oriented ferromagnetically along the short axis a, and no compensation for their ferromagnetic exchange interaction occurs. When the magnetic moments in the subsystems rotate relative to each other, the contribution from this exchange decreases. Thus, in the case that the magnetic moments are oriented in accordance with this magnetic structure, the collinear orientation of the magnetic moments in subsystems 1 and 2 is most probable.

Composition 2 [8] differs from our composition by the greatest displacement of iron ions to position 2c, according to work [8]. The same three structures as in the first case have minimal energies. The most favorable for the collinear orientation of the magnetic moments in the subsystems 1 and 2 is the structure (Fig. 3c). When the magnetic moments of the subsystems 1 and 2 are orthogonal, the magnetic structures Figs. 3a, 3b are the most profitable.

We assume that in the case where iron ions occupy predominantly position $4e_2$ with a small occupation of position 2c, magnetic ordering can occur like in Fe_3BO_5—in two stages. Most likely, the realized magnetic structure is similar to that obtained by Bordet for Fe_3BO_5 [3] (Fig. 3a).

As we noted earlier, position 2b is very weakly exchangeable with the others, and it is quite possible that the magnetic moments of copper ions in this position are ordered at a lower temperature than the magnetic moments of the remaining ions. This agrees with the experimental data obtained in [9].

Composition 3 [10] differs from the previous ones in that iron is predominantly in position 2c, in this case, the two magnetic structures shown in Fig. 5 are the most profitable.

In both structures, the antiferromagnetic order along the axis a is observed only in position 2c, in the remaining positions ordering of the moments along the short axis a is ferromagnetic. When the magnetic moments of one subsystem are rotated relative to the
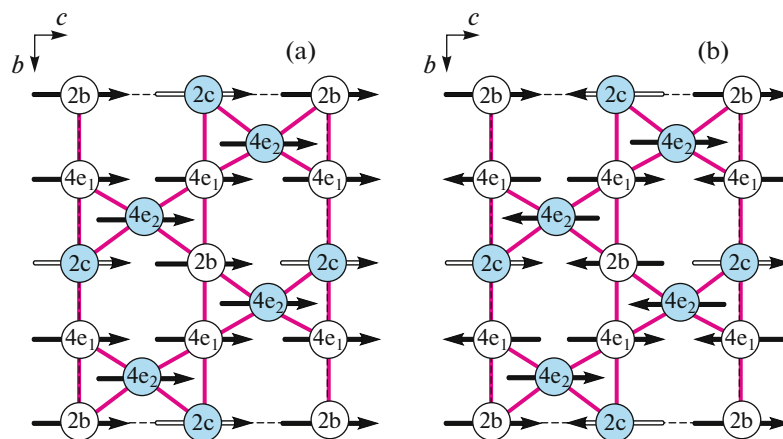
Fig. 5. (Color online) The most advantageous structures for composition 3 [10]: (a) FIM, (b) AFM5 (solid arrows show the FM orientation of the moments along the a axis, the dashed arrows show the AFM orientation of the moments along the a axis).

Table 9. The energies (in Kelvin) of magnetically ordered Cu_2FeBO_5 structures of composition 3 [10] with different orientations of the magnetic moments in the subsystems 1 and 2 relative to each other

2c	2d	$4e_1$	$4e_{1'}$	$4e_2$	$4e_{2'}$	$4e_3$	Type	$E\,(0°)$, K	$E\,(60°)$, K	$E\,(90°)$, K
↑↓	↓↑	↓↓↑↑	↓↓↑↑	↑↑↓↓	↓↓↑↑	↓↑↓↑	AFM1	−58	−58	−58
↓↑	↑↓	↓↓↑↑	↓↓↑↑	↓↓↑↑	↑↑↓↓	↑↓↑↓	AFM2	−66	−66	−66
↓↑	↓↑	↓↓↑↑	↓↓↑↑	↓↓↑↑	↑↑↓↓	↑↓↑↓	AFM3	67	63	60
↑↓	↓↑	↓↓↑↑	↑↑↓↓	↓↓↑↑	↓↓↑↑	↑↓↑↓	AFM4	−118	−97	−77
↑↓	↓↑	↓↓↑↑	↓↓↑↑	↓↓↑↑	↓↓↑↑	↑↓↑↓	AFM5	−189	−143	−97
↑↑	↓↓	↑↑↑↑	↑↑↑↑	↑↑↑↑	↑↑↑↑	↑↑↑↑	FIM	−192	−141	−90

other, the energies of both magnetic structures remain close, but the magnetic structure depicted in Fig. 5b become more profitable. Experimentally, both magnetic structures can be realized, however, the temperature dependence of the magnetization shows a very small value of the magnetization in the low-temperature region, which indicates that the magnetically ordered phase is most likely antiferromagnetic [18].

4. CONCLUSIONS

In this paper, we presented group-theoretical analysis and analysis of possible magnetic structures in the framework of the Anderson−Zavadsky model for Cu_2FeBO_5 at various distributions of iron ions among positions. For formulations, when iron ions occupy predominantly position $4e_1$, the most favorable is the magnetic structure, similar to that obtained by Bordet for Fe_3BO_5 [3]. The peculiarity of this structure is the compensated exchange interactions between the subsystems 4−2−4 and 3−1−3. Since the copper ions in position 2b are exchanged weakly with ions in position $4e_2$, and the exchange interactions with ions in position $4e_1$ and 2c are compensated, it is possible that magnetic ordering of copper at position 2b either does not occur or occurs at very low temperatures.

When iron ions occupy predominantly the 2c position, two magnetic structures are most profitable, which energies strongly depend on the mutual orientation of the magnetic moments in the subsystems. Unlike the other compounds, the ions in position 2b are exchange-related with other ions, due to the ferromagnetic orientation of the moments along the short axis a. In this case, the ordering is most likely in one stage, which agrees with the results of the experimental data [10].

REFERENCES

1. S. Sofronova and I. Nazarenko, Cryst. Res. Technol. **52**, 1600338 (2017).
2. J. P. Attfield, J. F. Clarke, and D. A. Perkins, Phys. B (Amsterdam, Neth.) **180−181**, 581 (1992).
3. P. Bordet and E. Suard, Phys. Rev. B **79**, 144408 (2009).
4. D. C. Freitas, C. P. C. Medrano, D. R. Sanchez, R. M. Nuñez, J. A. Rodríguez-Velamazán, and M. A. Continentino, Phys. Rev. B **94**, 174409 (2016).
5. D. C. Freitas, R. B. Guimarães, D. R. Sanchez, J. C. Fernandes, M. A. Continentino, J. Ellena, A. Kitada, H. Kageyama, A. Matsuo, K. Kindo, G. G. Eslava, and L. Ghivelder, Phys. Rev. B **81**, 024432 (2010).
6. C. P. C. Medrano, D. C. Freitas, D. R. Sanchez, C. B. Pinheiro, G. G. Eslava, L. Ghivelder, and M. A. Continentino, Phys. Rev. B **91**, 054402 (2015).
7. A. Utzolino and K. Bluhm, Z. Naturforsch. B **51**, 305 (1996).
8. K. Bluhm und J. Schaefer, Z. Anorg. Allgem. Chem. **621**, 571 (1995).
9. M. A. Continentino, J. C. Fernandes, R. B. Guimarães, H. A. Borges, A. Sulpice, J.-L. Tholence, J. L. Siqueira, J. B. da Cunha, and C. A. dos Santos, Eur. Phys. J. B **9**, 613 (1999).
10. G. A. Petrakovskii, L. N. Bezmaternykh, D. A. Velikanov, A. M. Vorotynov, O. A. Bayukov, and M. Schneider, Phys. Solid State **51**, 2077 (2009).
11. S. Sofronova, E. Moshkina, I. Nazarenko, Y. Seryotkin, S. Nepijko, V. Ksenofontov, K. Medjanik, A. Veligzhanin, and L. Bezmaternykh, J. Magn. Magn. Mater. **420**, 309 (2016).
12. O. A. Bayukov and A. F. Savitskii, Phys. Status Solidi B **155**, 249 (1989).
13. P. W. Anderson, Phys. Rev. **115**, 2 (1959).
14. G. A. Sawadtzky, W. Geertswa, and C. Haas, J. Magn. Magn. Mater. **3**, 37 (1976).
15. M. V. Eremin, Sov. Phys. Solid State **24**, 239 (1982).
16. O. A. Bayukov and A. F. Savitskii, Phys. Solid State **36**, 1049 (1994).
17. J. B. Goodenough, Phys. Rev. **117**, 1442 (1960).
18. C. Z. Tan, Phys. B (Amsterdam, Neth.) 269, 373 (1999).